

# 3-D Nonlinear Earthquake Response of R.C. Box Girder Bridges with Expansion Joints and Bearing Devices



**B. Tiliouine & M. Ouanani**

*Ecole Nationale Polytechnique, B.P. 183, Algiers, Algeria  
Laboratoire de Génie Sismique et de Dynamique des Structures, ENP*

## **SUMMARY:**

This paper summarizes the main results of an analytical investigation to study the nonlinear earthquake response of a reinforced concrete box girder bridge with expansion joints and bearings devices at abutments and to identify the most probable failure mechanism governing its collapse. In order to include the contribution of lateral ground motion components and to gain better insight into input ground motion effects on the nature of bridge failure mechanisms, a 3-D finite element model of the Mascara box girder bridge (North Western Algeria) is developed. The corresponding 3-D nonlinear dynamic analyses are performed for three major acceleration time histories covering a wide range of seismic hazard scenarios. A bilinear hysteretic model of plastic hinges at pier ends and nonlinear characteristics of expansion joints and bearing devices are established. Numerical results indicate that various types of failure mechanisms (ranging from localized damage to total collapse of the bridge) may take place depending on ground motion intensities including the contribution of lateral components. It is also conclude that in order to ensure an acceptably safe seismic performance of R.C. box girder bridges, particular attention should be devoted not only to appropriate assessment of rotational ductilities and drift demands at various damage states but also to proper evaluation of nonlinear mechanical characteristics of restrainers, bearing devices and potential plastic zones at pier ends at the design stage.

*Keywords: 3-D Seismic response, Box Girder Bridges, Abutment pounding, Restrainers failure, Bearing Device, Plastic hinges, Failure mechanisms.*

## **1. INTRODUCTION**

Highways bridges are key components of land transportation networks. They provide emergency links during earthquakes and there operability after major seismic events is essential. High seismic performance is generally required for these lifelines structures as their collapse lead often to loss of human lives and result in significant economic impacts. Thus, it is of crucial importance to be able to predict the failure mechanisms of the various components a given bridge in order to identify its overall failure mechanism of at collapse state and its corresponding time of occurrence under severe earthquake motion.

Even though considerable progress has been made in modeling and seismic analysis of R.C. bridges in the last few years, several cases of significant of bridge damages have been reported in past earthquakes (e.g. (Japanese Committee of Earthquake Engineering, 1996), (Basoz and Kiremidjian, 1998) and (Hamada et al., 1999)). Spectacular failures of bridges due to unseating of the decks at expansion joints resulting from restrainers failure, formation of plastic hinges at pier ends, excessive shear displacements of bearing devices as well as pounding phenomenon have been commonly observed in several major earthquakes. In addition, investigations of past and recent bridge damage data have illustrated that bridge structural performance may be very sensitive to intensities of earthquake ground motions (Banerjee and Shinozuka, 2008).

In this paper, the main results of an extensive numerical investigation on the dynamic progressive failure and subsequent collapse mechanisms of a typical R.C. box girder bridge with expansion joints and High Damping Rubber Bearings (HDRB) at abutments are presented. Full 3-D finite element modeling of the Mascara box girder bridge (North Western Algeria) is used in the study and comparative assessments of the nonlinear seismic response of the bridge system using 2D and 3D

ground motions with various probabilities of exceedence are carried out. Nonlinear bridge responses are discussed in terms of temporal variations of rotation ductility demands at pier ends, axial forces in restrainers, pounding forces at the interface of deck and abutment wall at expansion joints as well as shear strains at isolation abutment bearings. Finally, based on the numerical results obtained in the present study, conclusions of engineering significance are given.

## 2. BRIDGE MODELLING

### 2.1. Physical model

A typical R.C. box girder bridge, with expansion joints and bearings devices at abutments located in earthquake zone III of North Western Algeria is considered herein in order to illustrate its seismic response characteristics and the nature of bridge failure mechanism governing its collapse under severe earthquake ground motion. The bridge has an overall length of 216m and consists of three continuous spans in prestressed concrete with a mid-span length of 100m and two end spans of 58m length each as indicated in Fig. 1. a. The superstructure consists of a longitudinally R. C. deck, 9.50m wide with variable height, (see Fig. 1. b) and moment of inertia in accordance with the following expression:

$$I = I_0 \left( 1 + K \left( \frac{x - \alpha L}{1 - \alpha L} \right)^2 \right)^{\frac{5}{2}} \quad (1.1)$$

In this expression, K is a constant determined as follows:

$$K = \left( \frac{I_1}{I_0} \right)^{0.4} - 1 \quad (1.2)$$

where  $I_1$  represents the moment of inertia on pier and  $I_0$  the moment of inertia on abutment or middle of mid span. The parameter  $\alpha$  is equal to the ratio of end span length with constant cross section, ( $\alpha L$ ), to the total length (L) of the end span.

The geometrical properties of the bridge deck and piers are summarized in Table 1 below.

**Table 1.** Geometrical properties of the bridge deck and piers of Mascara bridge.

Sections	Cross-section (m2)	Torsional Inertia (m4)	Moment of inertia (m4)		Shear areas (m2)	
	A	I <sub>x-x</sub>	I <sub>y-y</sub>	I <sub>z-z</sub>	A <sub>z</sub>	A <sub>y</sub>
Segment on pier	8.12	43.21	43.26	43.22	4.46	3.54
Segment on abutment	6.17	11.38	6.64	31.98	4.63	1.73
Piers	4.5	13.43	14.93	6.29	3.06	1.8

Young's modulus and mass density of concrete are taken respectively as  $2.49 \times 10^{10}$  N/m<sup>2</sup> and 2500 Kg/m<sup>3</sup> with 5% damping at each mode of vibration.

The bridge is supported by two intermediate RC piers of equal height of 40m, with identical hollow rectangular cross sections, (see Fig. 1. c) and two rigid abutments at its end with unseating length equal to 0.70m. Expansion joints and high damping rubber bearing (HDRB) isolation bearings are located only at abutments. The footings are supported on pile foundations.

Details on the 3-D modal properties of the first three vibration modes for (symmetrical and unsymmetrical), longitudinal, vertical, lateral and torsional bridge mode shapes as well as modal intercorrelations can be found in reference (Tiliouine and Ouanani, 2011) whereby it was shown, among other things, that lateral mode of vibration was the most dominant.

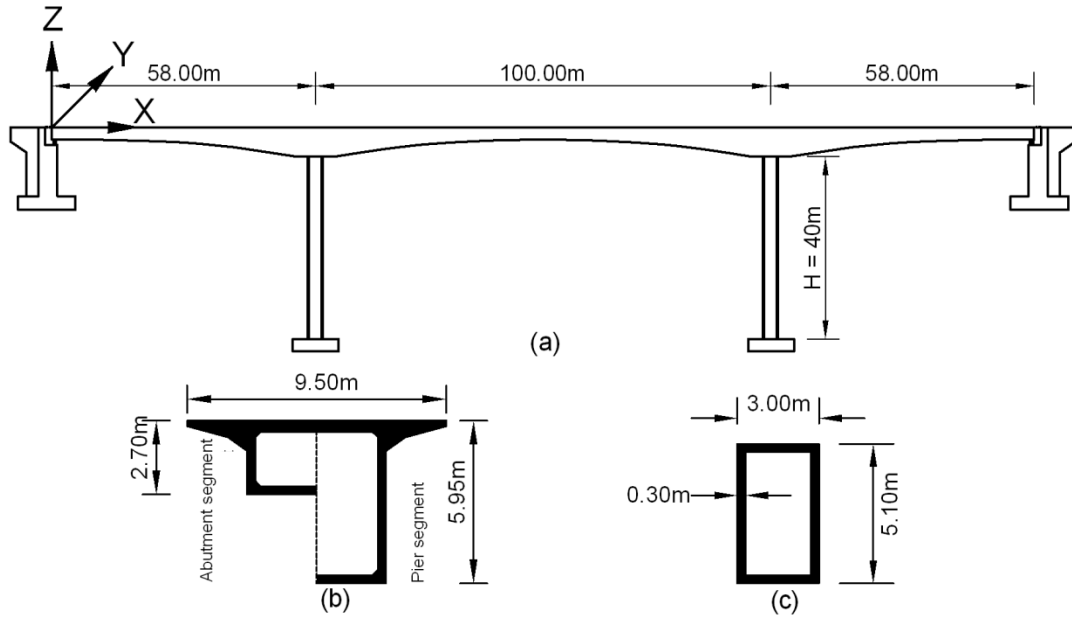


**Figure 1.** Description of Mascara Bridge: (a) Elevation of bridge, (b) Cross-section of segments, (c) Cross-section of piers

## 2.2. Non linear analytical model

The bridge has seat –type abutment which allows limited longitudinal movement of the superstructure due to the gap between the superstructure and the abutment back wall. The support provided by the abutment is assumed to be fixed against translation vertically, fixed against rotation about the longitudinal axis of the superstructure and has non linear translational springs in the longitudinal and lateral directions. The two shear degrees-of freedom system used for each of the two rectangular, HDRB bearings at each abutment is modelled by a bilinear model and based on three parameters, namely initial stiffness  $K_1$ , post-yield stiffness  $K_2$  and characteristic strength  $Q$ . The parameters values adopted in this study, in terms of effective stiffness  $K_{eff}$  and equivalent damping ratio  $\xi_{eff}$  for the pair of bearings in the longitudinal and lateral directions were defined for a design displacement of 0,15m and are given in Table 2.

**Table 2.** Bearing device properties.

Direction	$K_1$ (KN/m)	$K_2$ (KN/m)	$K_{eff}$ (KN/m)	$Q$ (KN)	$\xi_{eff}$
Longitudinal and Lateral	4702	933	1184	38,53	0,16
Vertical direction	$1790 \times 10^3$	-	-	-	-

The bridge piers are considered to be fixed at base against both translation and rotation ignoring, soil structure interaction. The seismic excitation of bridge generates bending moments in piers which may lead to the formation of plastic hinges at both pier ends. The nonlinear moment-curvature relationships at these plastic hinges have been established following the procedure given in reference (Priestley et al., 1996). For the sake of simplicity, however, bilinear rotational springs have been introduced to model for these potential plastic hinges, (see figure 2). All nonlinearities including expansion joints and bearing devices involved in the model are also shown in the same figure. The opening and closure of expansion joint during bridge movement under earthquake ground motion are modeled by introducing hook and gap elements, respectively. The hook element represents the effect of restrainer at expansion joint and controls relative displacement (excessive separation) between the superstructure and the abutment back wall. It is modeled by introducing a linear spring with stiffness  $K_{Hook} = 17 \times 10^2$  KN/m. An initial slack of 0.60m is provided in restraining cables and axial forces are generated when restrainers get engaged by loosing this initial slack. The gap element is provided to take care of pounding effects between the superstructure and the abutment back wall. This initial gap provided in

the gap element is 0.10 m and pounding develops the compressive forces at the interface of superstructure and abutment back wall when the relative displacement exhausts this initial gap width. It is modelled by introducing a linear spring with stiffness  $K_{Gap} = 17 \times 10^5$  KN/m.

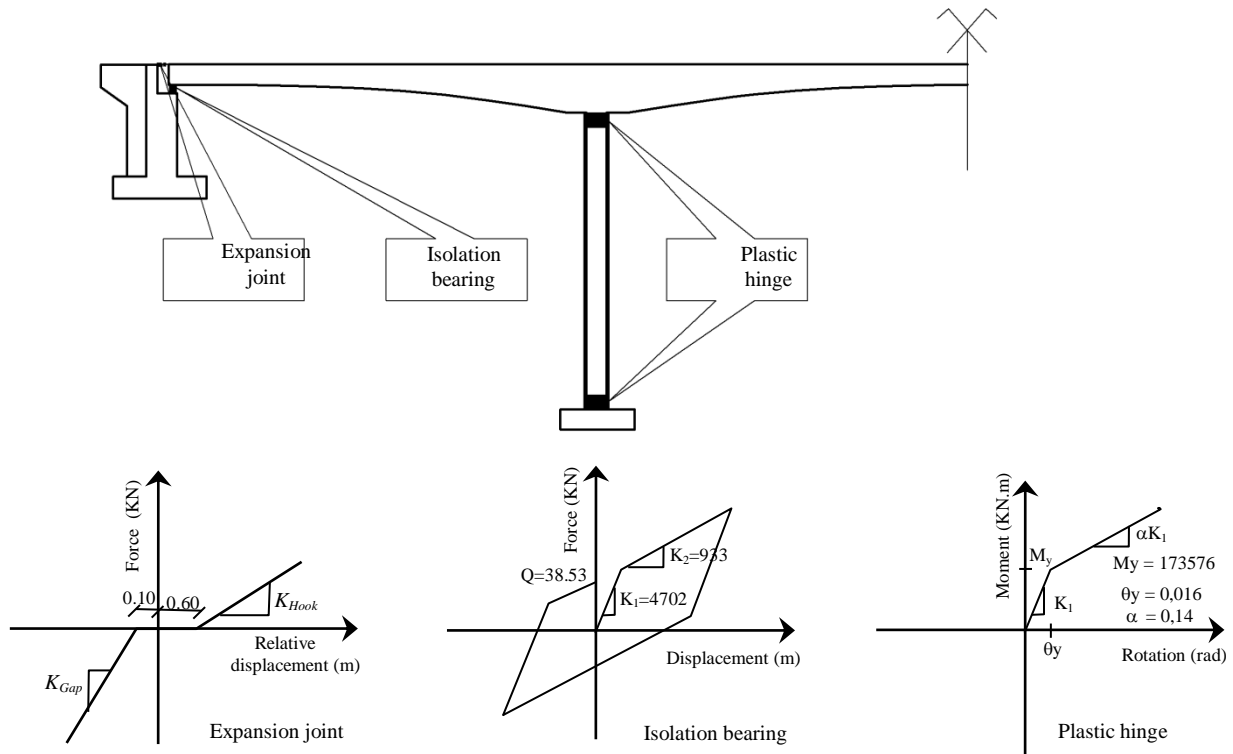


**Figure 2.** Non linear model properties of expansion joints, isolation bearings and piers for Mascara bridge.

The superstructure and substructure of bridge are modeled as a lumped mass system divided into a number of small discrete 3-D frame elements. Each adjacent element is connected by a node and at each node six degrees of freedom are considered; three translational in X - X, Y - Y and Z - Z directions and three rotational about these three axes (Zienkiewicz et Taylor, 2005). The entire bridge system is approximated analytically by the 3-D nonlinear FEM model presented in Fig. 3.

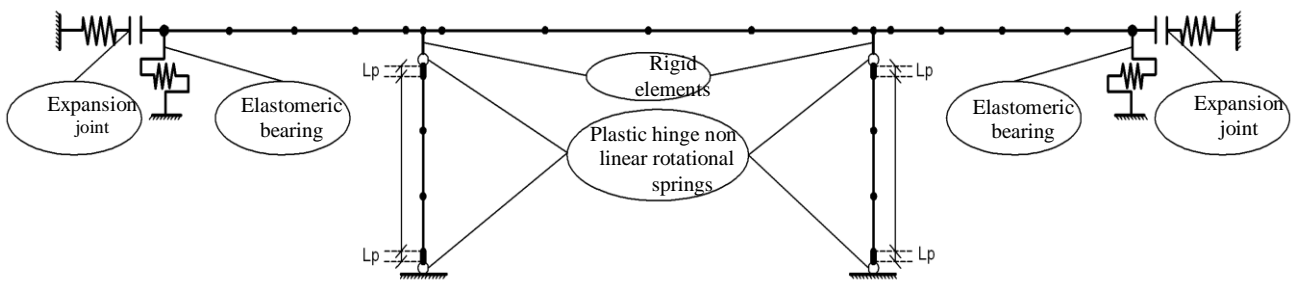


**Figure 3.** Three-dimensional nonlinear analytical model of Mascara bridge.

### 3. ANALYSIS SOFTWARE AND SEISMIC EXCITATIONS

3D nonlinear dynamic seismic response using 2D and 3D components of ground motions were carried out using general purpose FEM computer program SAP 2000 (Nonlinear version 15) as it is the most common and user friendly software by practicing engineers for nonlinear analysis of structures. The 3D dynamic analyses of bridge response were performed under 3 major acceleration time histories selected from the data base developed for the FEMA SAC project (Cf. <http://quiver.eerc.berkeley.edu:8080/studies/system/motions>). The numerical integration was carried

out using the Hilbert- Hughes-Taylor algorithm as implemented in SAP2000. The rationale behind the selection of the above mentioned seismic excitations lies in the statistical fact that they are derived from historical records (with some linear adjustments) and consist of 3 Groups (each consisting of 20 time histories) having return periods of 25, 475 and 72 years and are representative of earthquakes with probabilities of exceedence equal to 2%, 10% and 50% in 50 years time. These acceleration time histories are associated respectively with the strong 1994 Northridge California earthquake (which caused substantial damage to some 200 bridges), the 1994 El-Centro earthquake (with spectral characteristics known to closely approximate the design spectral shapes adopted by the UBC code on firm soil sites) and the 1979 Imperial valley earthquake which may be considered, for the purpose of this study, as a weak event. Thus, it may be considered that these accelerations time histories are derived from earthquake ground motion processes that cover a wide range of seismic hazards and can therefore be used for better understanding of global seismic performance and study of dynamic progressive failure mechanism of the study bridge. The 3D components of a typical acceleration time history belonging to each group are plotted in fig. 4 at the same scale for comparison purposes in terms of intensity, frequency content and strong motion duration characteristics.

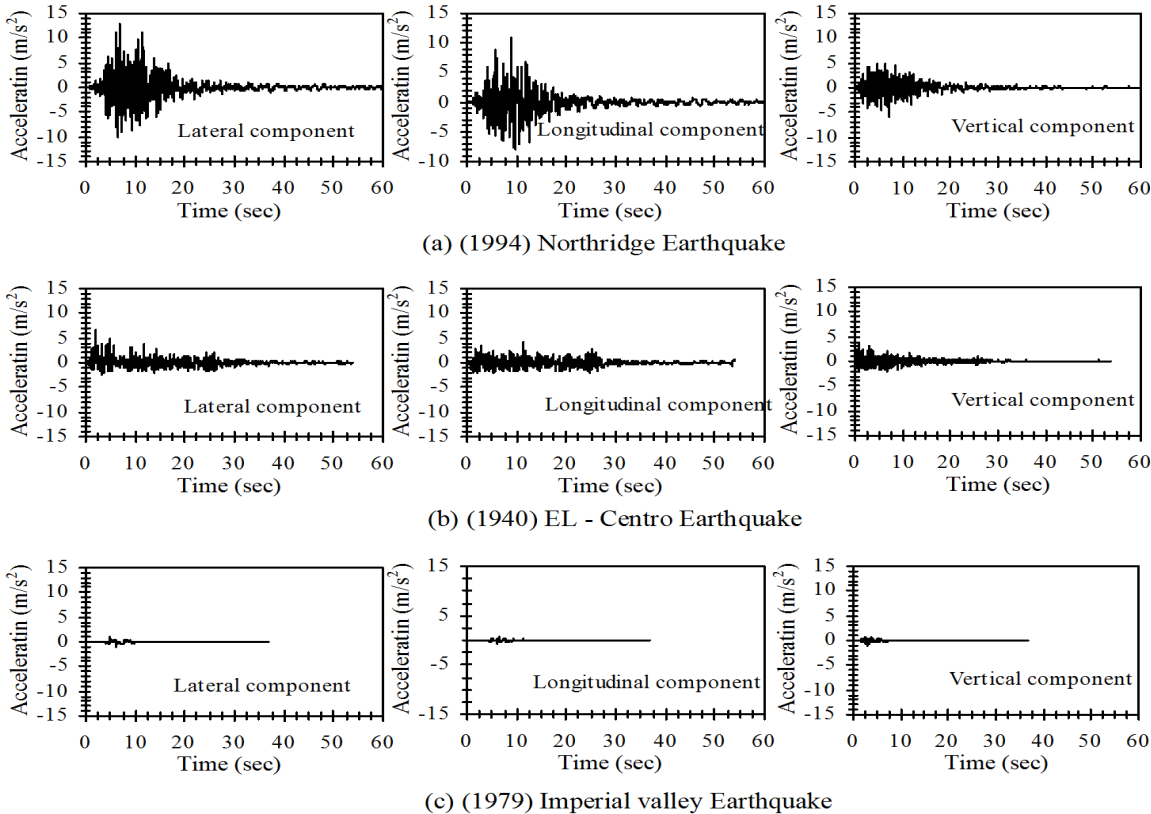


**Figure 4.** 3-D components of acceleration time histories used in present study.

**4. SEISMIC RESPONSES OF BRIDGE**

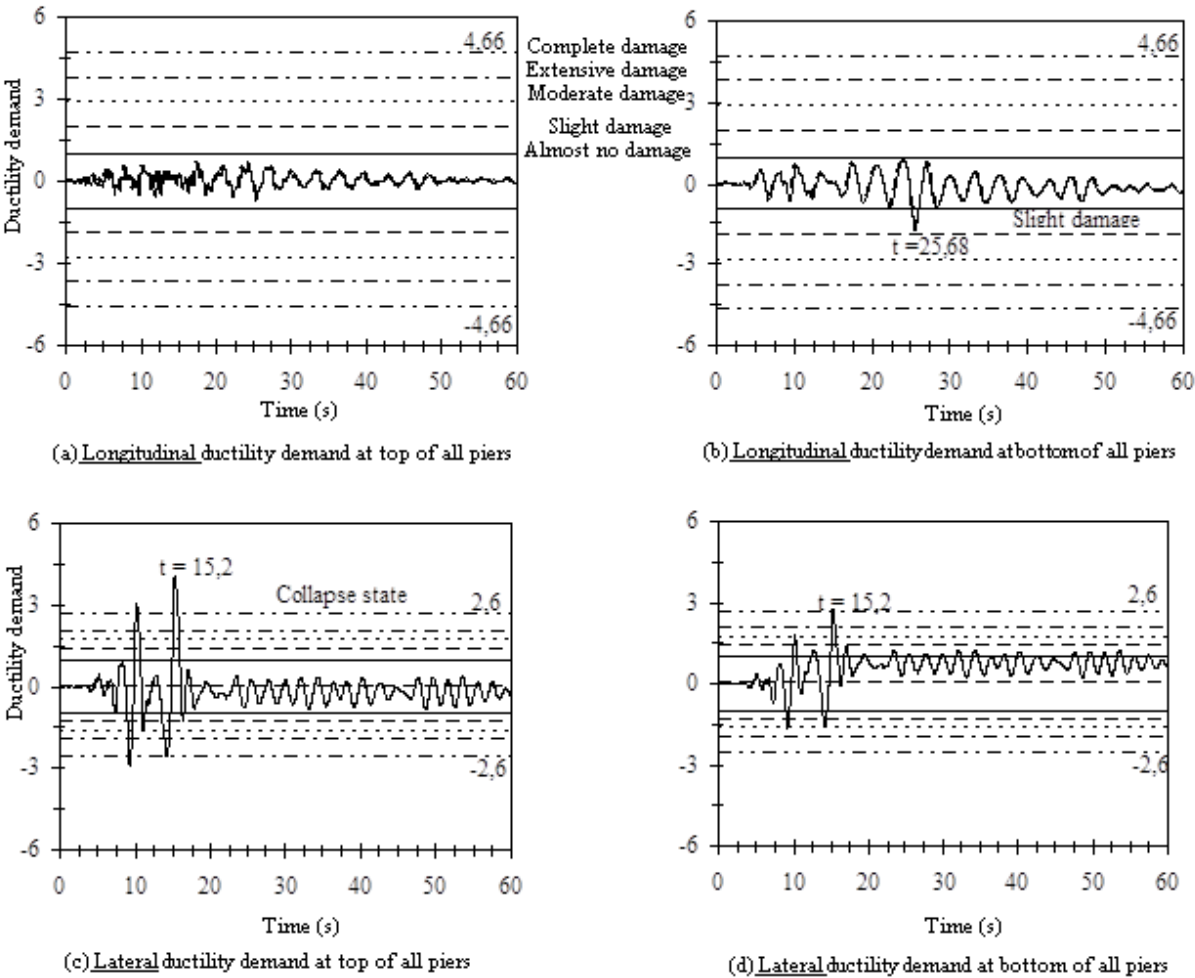
Most studies on fragility analysis of bridges use rotational ductility of piers as the primary damage measure. By definition, rotational ductility can be expressed as the ratio of rotation ( $\theta$ ) at pier end to its yield rotation ( $\theta_y$ ). In this study, the quantified damage state for the bridge piers with drift limits associated with five damage states ranging from yield state to collapse damage state have been established. Similarly, shear strain threshold values are utilized to capture the associated damage states in the HDRB isolation bearing devices. Following Dutta and Mander (1999), five different damage states can be defined based on the yield and ultimate curvatures obtained from moment-rotation plot shown in fig. 2. Table 3 illustrates the description of these five damage states and the computed ductility limits in the plastic zones formed at the end piers of Mascara bridge in both lateral and

longitudinal directions. Corresponding shear strain limits in isolation bearings are also reported in the same table.

**Table 3.** Definition of component level damage index of piers and bearings

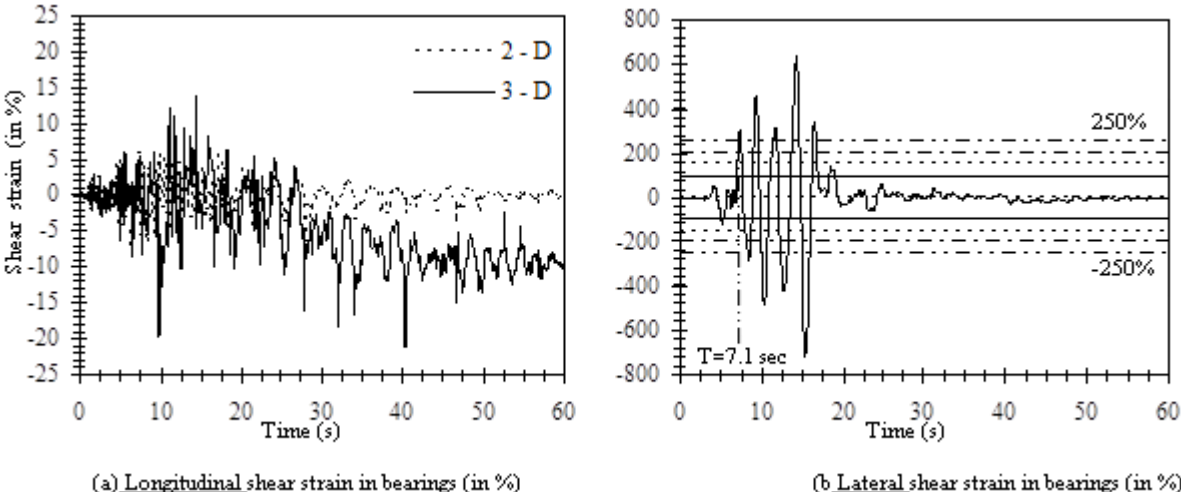
Damage state	Description	Piers			Bearings
		Drift Limits	Rotational ductility limits		Shear Strain ( $\gamma$ ) in %
			Lateral Direction	Longitudinal Direction	
Almost no	First yield	0.005	1.00	1.00	$\gamma < 100$
Slight	Cracking, spalling	0.010	1.34	1.91	$100 < \gamma < 150$
Moderate	Loss of anchorage	0.025	1.67	2.83	$150 < \gamma < 200$
Extensive	Incipient pier collapse	0.050	1,73	3.74	$200 < \gamma < 250$
Complete	Piers collapse	0.075	2.60	4.66	$\gamma > 250$

Fig. 4 below, shows temporal variations (in lateral and longitudinal directions) of rotation ductility demands at pier ends under Northridge 3-D acceleration time histories. It is noted that rotational ductilities at all pier ends have practically the same values as all piers have identical characteristics for a given direction. It is also seen that when 3-D seismic components are taken into consideration, failure mechanism leads to complete collapse of the bridge at 15,2s in the lateral direction when the rotational ductility demand at piers ends crosses the collapse state (i.e. rotation ductility capacity equal to 2,60) for all piers simultaneously.



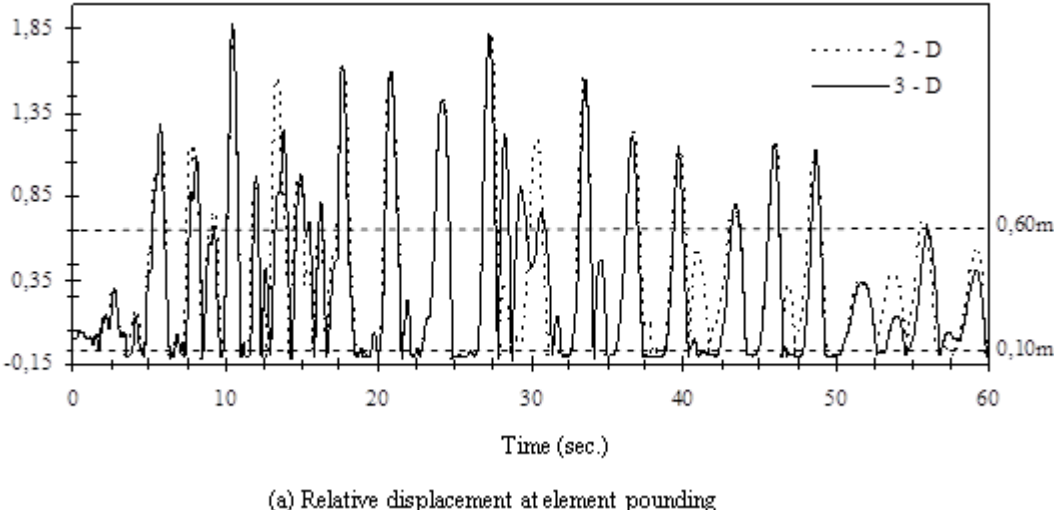
**Figure 4.** Rotational ductilities at pier ends of bridge model under Northridge earthquake

Fig. 5 below, shows shear strain time-history response of HDRB isolation devices at abutment back wall. It can be observed that including the lateral acceleration component has significant effect on shear strain responses of HDRB isolation devices in both lateral and longitudinal directions.

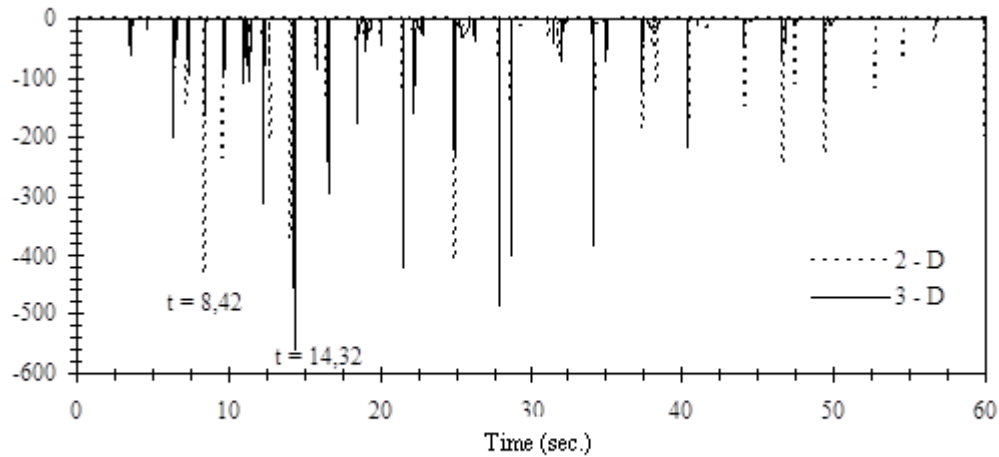


**Figure 5.** Shear strain of HDRB bearing devices at abutments of bridge model under Northridge acceleration times histories

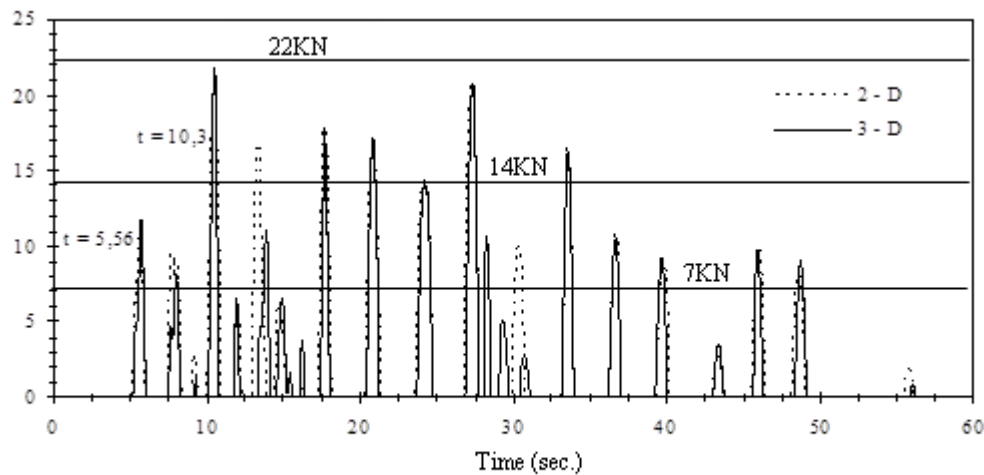
For the same ground motion, the relative displacement time history at the two ends of expansion joints is plotted in Fig. 6.a. Impact force develops at the bridge deck and abutment back wall when they come into contact by exhausting the initially provided gap and hence by causing pounding. Fig. 6.b depicts that pounding force generates only at those time instants when relative inward movement between deck and abutments exceeds the specified value (0.10m). The bridge experiences a maximum of 557, 96 kN impact force at  $t = 14.32s$  when including lateral ground motion component (versus 430.64kN at 8.42s when using longitudinal and vertical components only). The outward movement of the superstructure and the abutment back wall at the expansion joint results in the development of the axial force in restrainers when the hook element gets engaged by losing initially provided slack of 0.60m. Fig. 6.c shows the development of axial force in the restrainers. This axial force is transmitted to the nearby concrete block through anchors that hold the restrainer in position. These anchors fail when the axial force exceeds the anchor capacity and this failure is assumed conservatively to lead to the collapse of bridge. Depending on the design capacity, however, the restrainer itself fails before anchorage failure. This also may be considered to result in the bridge collapse.



**Figure 6.** Relative displacement and maximal forces at expansion joint at abutment (Northridge earthquake) (continues)



(b) Pounding force developed at expansion joint



(c) Axial force in restrainer (Northridge)

**Figure 6.** Relative displacement and maximal forces at expansion joint at abutment (Northridge earthquake)

In Table 4, computed maximal shear strain values at abutment bearings (using 2D and 3D) ground motion components in bridge lateral and longitudinal directions are summarized for three selected events.

**Table 4.** Maximum shear strain at abutment bearings (in %)

Element	Restrainer cable		Impact element	
	2-D (KN)	3-D (KN)	2-D (KN)	3-D (KN)
Scaled seismic components				
1994 Northridge	20,87	21,89	430,64	557,96
1940 El Centro	15,22	15,24	276,77	283,86
1979 Imperial Valley	1,62	1,65	105,15	181,39

It is seen that maximal shear strain responses using 2D and 3D components ground motions are significantly different in both lateral and longitudinal bridge directions. These effects are less pronounced for ground motions having higher probabilities of exceedence (i.e. with lower intensities).

Table 5 shows maximal forces at expansion joints at abutments. Similar values of maximal forces in restrainer cables are obtained when using lateral ground motion components. However, significant

difference in maximal pounding forces are observed when 3D ground motion components are used.

**Table 5.** Maximal forces at expansion joint at abutment

Scaled seismic components	Lateral direction		Longitudinal direction	
	2-D	3-D	2-D	3-D
1994 Northridge	0	716,52	7,55	13,77
1940 El Centro	0	309,58	5,22	7,05
1979 Imperial Valley	0	92,61	1,77	1,96

Table 6 below, gives maximum ductility demands of plastic hinges at column ends for bottom and top piers of Mascara bridge when using 2D and 3D ground motion components. It is observed that maximal ductility demand responses using 2D and 3D components ground motions are significantly different in lateral direction for the bottom piers. However, in longitudinal direction, values of maximal ductility demands of plastic hinges are seen to be very close when using 2D and 3D components ground motions. Similar trends are observed in top piers.

**Table 6.** Maximum ductility demand of plastic hinge at column ends of bridge

Scaled seismic component	Bottom piers				Top piers			
	Lateral direction		Longitudinal direction		Lateral direction		Longitudinal direction	
	2 - D	3 - D	2 - D	3 - D	2 - D	3 - D	2 - D	3 - D
Seismic components	2 - D	3 - D	2 - D	3 - D	2 - D	3 - D	2 - D	3 - D
1994 Northridge	0	2,736	1,792	1,787	0	4,084	0,746	0,750
1940 El Centro	0	0,688	0,832	0,831	0	0,849	0,433	0,431
1979 Imperial Valley	0	0,250	0,153	0,153	0	0,305	0,099	0,099

All the above mentioned failure mechanisms can lead to bridge collapse at the exception of pounding and bearing failure mechanisms which may be considered as localized damages. By definition, it is considered that complete bridge collapse with the shortest time of occurrence controls the governing failure mechanism. However, it should be noted that the governing failure mechanism changes as restrainer capacity varies. For example, if the restrainer is assigned to a design capacity of 7KN or less, bridge collapses due to the failure of restrainer or anchorage at time  $t = 5.56$ sec. This scenario changes for a different restrainer capacity. For restrainer capacity of 14KN, bridge collapses again due to failure of restrainer or anchorage, at time  $t = 10.3$  sec resulting in unseating failure and subsequent collapse. However, for restrainer capacity 22KN or more, plastic hinges form at  $t = 15.2$  sec at all pier ends simultaneously resulting in total collapse of bridge.

## 5. CONCLUDING REMARKS

In this paper, the main results of an extensive numerical investigation on the 3-D seismic progressive failure and the anticipated overall bridge failure mechanism of a typical R.C. box girder bridge with both HDRB isolation bearings and expansion joints at abutments, are presented. To this end, full 3-D FEM modeling of the Mascara bridge (North Western Algeria) is used and comparative assessments of nonlinear dynamic responses of the bridge system using 2-D and 3-D ground motions covering different seismic hazard scenarios are carried out. The effects on the global bridge response of material nonlinearities characterizing the seismic behavior of various bridge components (including plastic hinges at pier ends, expansion joints and bearing devices) are considered simultaneously. Bridge responses are discussed in terms of temporal variations of rotation ductility demands at pier ends, axial force in restrainer, pounding force at the interface of deck and abutment back wall and shear strain at HDRB isolation bearings. From the numerical results obtained in this study, the following conclusions can be drawn:

- Moment-rotation relationships for plastic zones at pier ends of Mascara R.C. bridge (North Western

Algeria) and associated rotational ductility limits consistent with five damage states, ranging from yield to collapse, have been established.

- Various types of failure mechanisms ranging from localized damage to total bridge collapse may take place depending mainly on the input ground motion characteristics used for bridge analysis. To prevent deck unseating resulting from restrainers' failure and subsequent bridge collapse, particular attention should also be given to proper design of nonlinear characteristics of restrainers and bearing devices.
- A comparative assessment of nonlinear seismic bridge responses using 2D and 3D ground motion components shows that under this study:
  - i) The computed maximal shear strain responses are significantly different in the lateral and longitudinal bridge directions. These effects are more pronounced for higher intensities of ground motions.
  - ii) Significant differences in maximal pounding forces and times of occurrence are observed when all 3-D ground motion components are used.

It follows that in order to ensure an acceptably safe structural performance of a R.C. box girder bridge with expansion joints and isolation bearings at abutments, due consideration should be given at design stage to:

- An appropriate assessment of expected 3-D seismic design ground motions at constriction site.
- A proper estimation of rotational ductility and drift limits of bridge piers at the five damage states in both longitudinal and lateral directions.
- A sound evaluation of distortion limits of isolation bearings at abutments and restrainers capacities at expansion joints.

## REFERENCES

- Banerjee, S. and Shinozuka, S. (2008). Mechanistic Quantification of RC Bridge Damage Statistics Under Earthquakes Through Fragility Analysis. *Probabilistic Engineering Mechanics*. **23**, 12–22.
- Basoz, N. and Kiremidjian, A. (1998). Evaluation of Bridge Damage Data From the Loma Prieta and Northridge Earthquakes. *Technical report MCEER- 98- 0004, Multidisciplinary Center for Earthquake Engineering, State University of New York Buffalo, NY, USA.*
- Committee of Earthquake Engineering. (1996). The 1995 Hyogoken-Nanbu Earthquake, Investigation into Damage to Civil Engineering Structures. *Japan Society of Civil Engineers.*
- CSI, csiBridge. (2012). Computer and Structures. Inc. SAP2000 (Nonlinear version 15), *Nonlinear User's Manual Reference*, Berkeley, CA, USA.
- Dutta A. and Mander, JB. (1999). Seismic Fragility Analysis of Highway Bridges. *Proceedings of The Center-to-Center Project Workshop on Earthquake Engineering Frontiers in Transportation Systems*. p. 311–325, Tokyo, Japan.
- Hamada, M., Nakamura, S., Ohsumi, T., Megro, K., and Wang, E. (1999). The 1999 Ji-Ji Taiwan-Earthquake: Investigation into Damage to Civil Engineering Structures. *Japan Society of Civil Engineers.*
- Priestley, M.J.N, Seible F. and Calvi, G.M.S. (1996) .Seismic Design and Retrofit of Bridges, John Wiley & Sons, N. Y., USA.
- Tiliouine, B. and Ouanani, M. (2011). Réponse Sismique 3-D d'un Pont-Caisson à Inertie Variable. *Proceedings of the 8<sup>th</sup> French National Conference on Earthquake Engineering: Dynamic and Vibratory Aspects in Civil Engineering, AFPS 2011*, Paris, France.
- Zienkiewicz O.C. and Taylor R.L. The Finite Element Method, Solid Mechanics. 6<sup>th</sup> Edition, Vol. 2, 2005.